

Improving the Properties of the Porous Polylactic Acid Scaffold by Akermanite Nanoparticles for Bone Tissue Engineering

Masoud Arastouei ^{1,*}, Mohammad Khodaei ², Sayed Mohammad Atyabi ³, Milad Jafari Nodoushan ⁴

¹ Department of Biomedical Engineering, Central Tehran Branch, Islamic Azad University, Tehran 13185/768, Iran

² Department of Materials Science and Engineering, Golpayegan University of Technology, Golpayegan, Iran

³ Department of Nano Biotechnology, Pasteur Institute of Iran, Tehran, Iran

⁴ Hard tissue engineering research center, tissue engineering and regenerative medicine institute, central Tehran Branch, Islamic Azad University, Tehran, Iran

ARTICLE INFO

Article history:

Received 27 April 2020

Accepted 5 May 2020

Available online 15 September 2020

Keywords:

Akermanite

Polylactic acid

Fused deposition modelling

Scaffold

ABSTRACT

Bone tissue engineering serves as a solution to repair and rebuild the damaged bone. In this study, first, the akermanite nanoparticles were synthesized by the sol-gel method; then the polylactic acid (PLA) scaffold was made using the fused deposition modelling (FDM), and the akermanite nanoparticle booster was used to improve its properties. The image of the transmission electron microscopy (TEM) from akermanite particles showed that the size of these particles was 100 nm. The microstructure and phases of the scaffold was examined using scanning electron microscopy (SEM) and X-ray diffraction (XRD). The results of the field emission electron microscopy (FESEM) and energy dispersive spectroscopy (EDS, map) showed that the nanoparticles had a uniform distribution in the polymer matrix.

The results of the compression test also revealed that the addition of akermanite nanoparticles improved the strength of the polymer scaffold. The bioactivity test was performed by immersing the scaffolds in the simulate body fluid (SBF) and then was examined using (SEM). Formation of the hydroxyapatite crystals on the surface of the scaffold containing akermanite nanoparticles, showing that the addition of akermanite particles improved the bioactivity and mechanical properties of the scaffold; therefore, this scaffold could be a good choice for use in bone tissue engineering.

1-Introduction

Tissue engineering is a combination of engineering and life sciences; it is designed to provide a suitable structural scaffold for repairing, protecting, or enhancing the tissue functions. Scaffold, cells and food, along with oxygen, form the three vertices of the tissue

engineering triangle. From the perspective of tissue engineering, three-dimensional scaffolding for bone regeneration must mimic the biological and mechanical properties of the extracellular matrix (ECM) in order to control cell and bone functions [1]. In addition, high interconnectivity is essential for the transport of

* Corresponding author:

E-mail address: m.arastouei@gmail.com

oxygen and nutrients into the scaffold. To apply this method, the average size of the scaffolding pores should be in the range of 300-400 micrometers to allow the growth of steons in the scaffold [2, 3].

Fused deposition modelling (FDM) method for making porous scaffolds with the ability to control internal / external architecture is attractive due to its high flexibility in working with materials, low cost and good mechanical properties [4]. Polylactic acid (PLA) is a degradable, biocompatible, non-toxic and environmentally-friendly polyester that has recently been developed for the preparation of the PLA scaffold using the FDM method [9-5 [3,10, 11]. The interaction of the polymer with the cells must be improved due to its non-hydrophilicity, low surface energy, lack of detectable signals for the cell for implantation and cell migration, and its low compressive strength.

In this regard, the addition of bioactive mineral fillers to the degradable polymers for the manufacture of composite scaffolds is common. Polyester / silicate scaffolds are very suitable for the production of bone tissues. In such scaffolds, suitable mineral fillers can not only strengthen the mechanical properties of the scaffold, but also play an important role in strengthening cell adhesion, cell proliferation and differentiation [12]. In addition, bioactive fillers are able to neutralize destructive acidic products to prevent the inflammatory response and facilitate the formation of the bone-calcium phosphate interface layer [5]. However, fillers are not homogeneously distributed due to the large difference in their surface tension [6]. Silica-based glass-ceramic has received much attention due to its mechanical and bioactive properties. Akermanite ($\text{Ca}_2\text{MgSi}_2\text{O}_7$) is a silica-based bioactive glass that increases its hardness and density. In addition, the content of Ca, Mg, and Si of akermanite has been shown to increase the calcium deposition and differentiate adult stem cells, producing mature osteoblasts. The release of the silicon ions can stimulate regression. Akermanite can also be closely bond to the rabbit bone tissue [5, 12]. Zanetti et al. examined the bone mineralization behavior of pure akermanite scaffolds and composite with poly caprolactone, pure β -TCP scaffold and composite with poly caprolactone and found that akermanite scaffolds had better calcium deposition and osteocalcin expression [10]. Deng et al. Investigated the PLA-

akermanite composite scaffolds. Their results showed that the addition of akermanite, increased the scaffold strength [6]. In addition, ionic products released from akermanite neutralize the acidic products caused by the degradation of PLA. Akermanite also improves the adhesion, proliferation and differentiation of MC3T3-E1 cells due to the release of calcium, magnesium and silicon ions. Corcione et al. Prepared PLA- HA scaffold by mixing the two materials by extrusion and FDM methods [11]. The addition of 50% HA caused the polymer structure to become completely amorphous, which increased the absorption rate. It also reduced the compressive strength by increasing the porosity percentage. Studies focusing on akermanite mixing in the composite scaffolds are limited; so, in-depth studies are needed to clarify and validate akermanite reinforced composite scaffolds [13].

In this study, as a step towards the development of 3D printed scaffolds for bone tissue engineering, PLA composite filaments containing akermanite were investigated for the production of porous samples using the FDM technology. Porous scaffolds were studied in terms of structure, mechanical strength and bioactivity. A literature review showed that the PLA-akermanite composite has not been made by the fused deposition modelling, and this study is the first effort to investigate its processability.

2- Materials and methods

Polylactic acid was purchased from Sigma-Aldrich: GF45989881 with an average molecular weight of 10,000.

Akermanite (Ak) nanoparticles were synthesized by the sol-gel method. First, tetraethyl orthosilicate (TEOS), deionized water and normal nitric acid (HNO_3) were mixed by a magnetic stirrer at a molar ratio of 1-8-0.16 for 30 minutes; then, tetra ethyl orthosilicate and magnesium nitrate hydrate ($\text{Mg}(\text{NO}_3)_2 \cdot 6\text{H}_2\text{O}$) and hydrated calcium nitrate ($\text{Ca}(\text{NO}_3)_2 \cdot 4\text{H}_2\text{O}$) were added to the tuber solution at a molar ratio of 2-1-2 and mixed for further 2 hours. After gelling, the resulting material was dried in an oven at 80. C for 24 hours.

2-1- Preparation of the PLA / Ak scaffold

First, 50 cc of chloroform was poured into the Erlenmeyer flask at room temperature and polylactic acid was gradually added to it, while the solution was stirred with a magnet at a rate

of 200 rpm. The resulting solution was stirred for 3 hours using a magnetic stirrer to dissolve the polymer and obtain a uniform solution. On the other hand, the nano-particle akermanite powder was poured into another Erlenmeyer flask containing 200 cc of chloroform. The resulting mixture was stirred using a bath ultrasonic device (Grant XB6: UK) for 10 minutes to separate the nanoparticles and disperse the solution. The resulting suspension was immediately added to the mixing polymer solution and dripped; then stirring was done for 30 minutes to obtain a uniform mixture of polymer and nanoparticles. The resulting mixture was immediately poured into a steel container and poured at room temperature until it was completely dried. The percentage of akermanite nanoparticles in the scaffold was 20% by weight. These composites were then melted using the micro extruder (AES Lab-30: Aysa Machine, Istanbul, Turkiye), and 1.75 mm diameter filaments were prepared to be sent to a 3D printer. The filament was then machined using a 3D printer (FDM: Prusa i3 MK3) scaffold with 70% volumetric porosity. For printing, a nozzle with the diameter of 400 micrometers, the thickness of 400 micrometers per layer, the temperature of 210 °C, and the speed of 10 mm/s were used.

2-2- X-ray diffraction test (XRD) of akermanite particles

To prove the formation of the akermanite phase, as well as determining the size of its crystals, X-ray diffraction (XRD) patterns of the synthesized particles were used. The size of the particle crystals was determined using the Scherrer-Deby relationship. This relationship is defined as equation 1 [16-14]:

$$\text{Equation 1: } t = 0.9 \lambda / (B \cos\theta)$$

Here, t is the size of the crystals, λ is the wavelength of the radiation used in the test, B is the peak width at half height of the tallest peak, and θ is the angle of the tallest peak. X-ray diffraction spectrometer (PHILIPS (X'Pert-MPD)) with a copper target, with the wavelength $\lambda = 1.54\text{\AA}$ were used. The step size was selected to be 0.05 and the scattering angle range was 10-60. The operating voltage was 30 kV and the current was 30 mA. The X-ray diffraction patterns obtained were compared with the information in the standard cards by X'Pert HighScore software; by comparing the angles and intensities of the scatter peaks, the phases in the sample were determined.

2-3- Image of the electron microscopy (TEM) of the akermanite particles

In order to study the morphology and measure the size of the akermanite powder particles prepared in different conditions, the transmission electron microscopy (TEM: LEO 912 AB) at a potential difference of 200 kv was used. The transmission electron microscope provided a direct image of the nanoparticles and their size distribution.

2-4 Structural studies of the PLA / Ak scaffold using scanning electron microscopy (SEM) and energy dispersive spectroscopy (EDS, map)

The structure of the scaffolding was examined using scanning electron microscopy (SEM). For this purpose, the surface of the samples was first coated with gold using a sputter coater. To study the structure, a sample of each compound was selected and the surface structure of the scaffold prepared by scanning electron microscopy (SEM: Philips XL30) was investigated. The structure under study included morphology, size and distribution of pores, as well as the interconnectivity between scaffold pores. Also, in order to study the distribution of the nanoparticles in the structure of the composite scaffold, the energy dispersive spectroscopy was performed (EDS, map) of the silicon element.

2-5- Compressive strength test

To investigate the mechanical properties of the composite scaffold, a compression test, according to the ASTM F2150-19 standard, with a jaw speed of 0.5 mm / min was used on the samples with the dimensions of 10×10×10 mm at the ambient temperature. For this evaluation, HOUNSFIELD (H30KS) device was used and the stress-strain engineering diagram of the samples was drawn and the necessary information was extracted from them. This test was repeated 3 times for each sample and the mean values were reported.

2-6- Immersion of the scaffold in the simulated body fluid (SBF)

The bioactivity test is usually performed by immersing the samples in the SBF. The amount of hydroxyapatite formation on the surface of the sample serves as the criterion for bioactivity. In this study, the formation of the calcium phosphate layer on the surface of the PLA/Ak

composite scaffold due to immersion in the SBF liquid with a concentration of elements similar to that of human blood plasma was done with the formulation and method provided by Kokubo et al., according to the ISO/FDIS 23317 standard [17].

To perform the bioactive test, the specimens 5×5×5 mm were separated from the primary scaffold. All samples were immersed at the ambient temperature in a stationary SBF liquid [17]. The SBF was changed once daily. Samples were removed 7 days after immersion in the SBF. After removing the SBF liquid, the samples were rinsed several times with ionized water and then dried in a vacuum oven for two days. The formation of apatite on the surface of the scaffold was investigated using the scanning electron microscopy (SEM: Philips XL30).

3. Results and discussion

3-1- Microstructure observation

Figure 1 shows the image of the transmission electron microscope (TEM) and the X-ray diffraction pattern of akermanite particles. As can be seen, the synthesized particles were about 100 nm in semi-spherical shape.

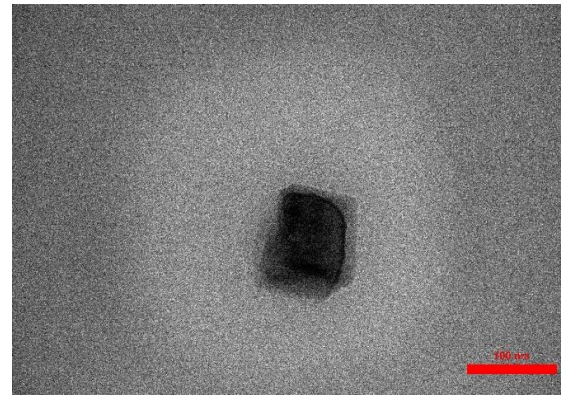


Fig. 1. Transmission electron microscopy (TEM) image of the akermanite nanoparticles.

3-2- X-ray diffraction pattern

The X-ray diffraction peaks of akermanite nanoparticles, polylactic acid polymer (PLA) and PLA-Ak composite are presented in Figure 2. It could be observed that the peaks of the X-ray diffraction pattern of akermanite nanoparticles, both in terms of intensity and position, were in a good agreement with the standard akermanite card 0046-087-01 (all peaks belong to akermanite), showing that the akermanite phase was formed with high purity.

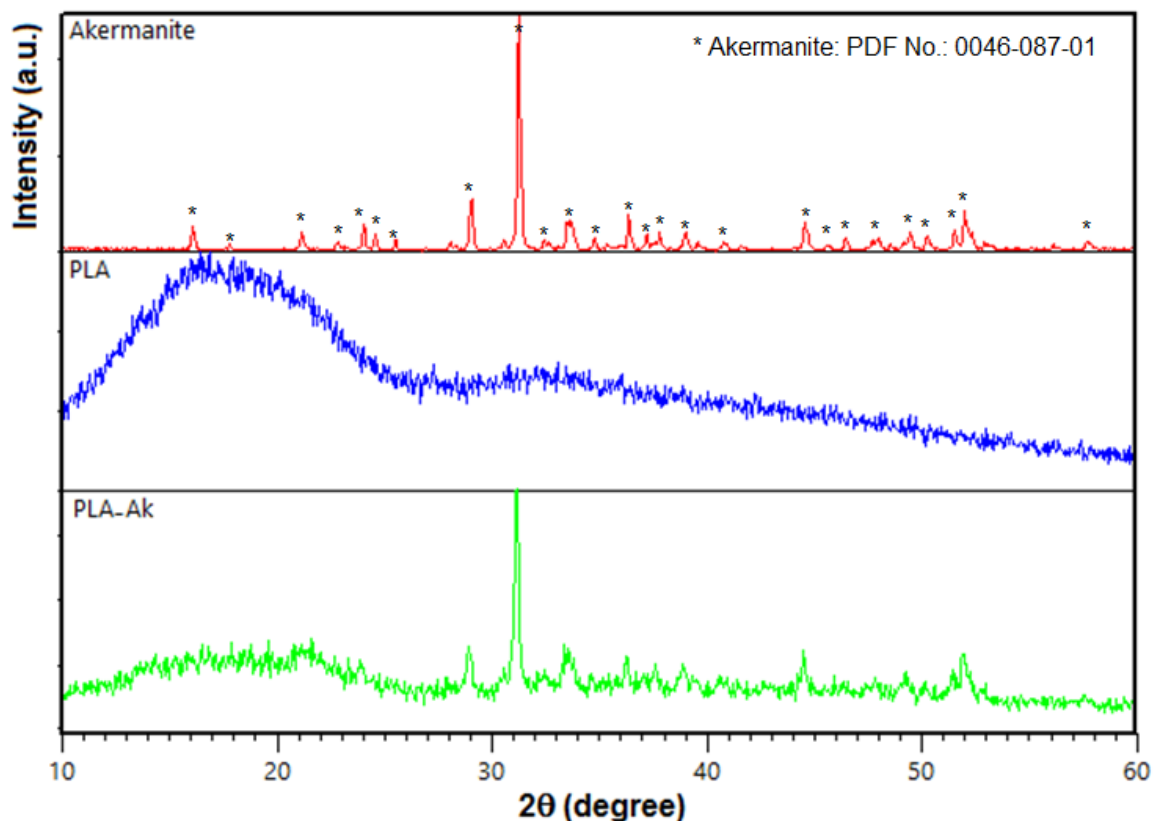


Fig. 2. X-ray diffraction pattern of akermanite nanoparticles, polylactic acid polymer (PLA) and the PLA-Ak composite.

The size of the synthesized particles was also calculated, which was about 54 nm, corresponding to the particle size seen in the images of the transit electron microscope (TEM). Comparing the patterns of the PLA and PLA-Ak scaffold showed that polylactic acid polymer consisted of a wide peak in the range of 10-25 degrees, indicating that some parts of the polymer was amorphous. Also, the height of polylactic acid peaks was decreased with the addition of nanoparticles. This suggested that the addition of akermanite nanoparticles reduced the polylactic acid crystallinity.

3-3- Structural studies of PLA / Ak scaffolds using scanning electron microscopy (SEM) and energy dispersive spectroscopy (map)

Figure 3 shows a scanning electron microscope (SEM) image of a scaffold made of pure polylactic acid and the scaffold containing

akermanite nanoparticles. As can be seen, the scaffold had regular and interconnected open cavities, so that the internal connection between the cavities inside the scaffold was established. This structure would be suitable for tissue engineering because the internal connection of the cavities in a scaffold for the penetration of oxygen and nutrients into the scaffold and the disposal of waste from metabolic activity could be an important feature of the scaffold. On the other hand, the size of the scaffold holes was about 200-200 μm , which could be suitable for bone tissue engineering. In terms of appearance, cracks and discontinuities were not observed on the surface of the scaffold. The microstructures of both PLA and PLA-Ak scaffolds were similar and there was no significant difference; acrimony had no negative effect on the quality of 3D printing.

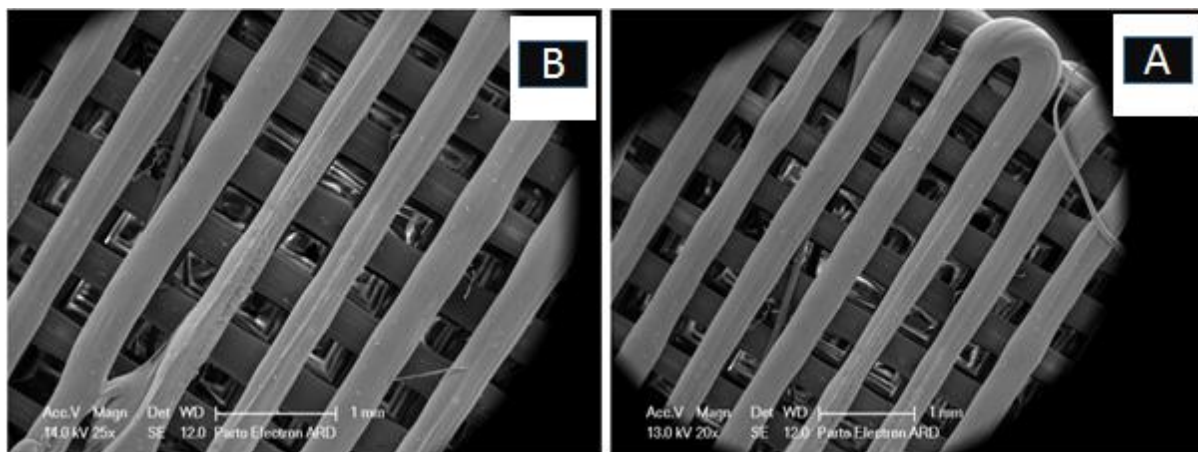


Fig. 3. Scanning electron microscopy (SEM) image of the surface of the nanocomposite scaffold: A) PLA and B) PLA-Ak.

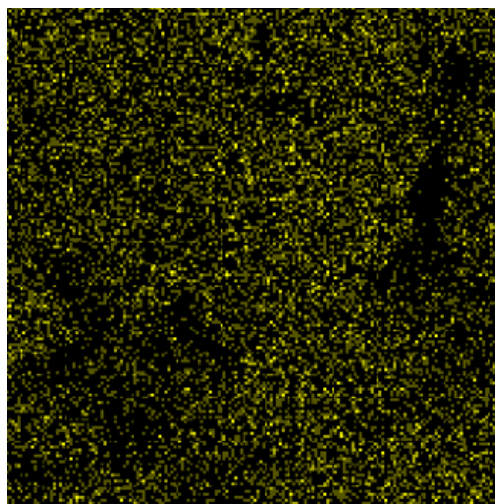


Fig. 4. Energy dispersive spectroscopy (EDS, map) of the silicon element in the PLA-Ak scaffold.

To investigate the distribution of akermanite nanoparticles in the PLA-Ak composite, energy dispersive spectroscopy (EDS, map) of the silicon element (the main component of akermanite) was performed by the EDS detector connected to the FESEM device; its results are shown in Figure 4. As can be seen, the element was uniformly distributed in the scaffold structure. This suggested that despite the possibility of the agglomeration of some nanoparticles, their distribution throughout the scaffold was appropriate; so, this could improve the bioactivity and other properties of the scaffold, such as mechanical properties and the cellular behaviour.

3-4 Compressive strength

To test the strength, the scaffold was tested by compression test. The engineering stress-strain curve obtained from the compression test for the PLA and PLA-Ak scaffolds is shown in Figure 5. As can be seen, the stress-strain curve of engineering had a flat stress area that was located after the delivery point. The flat stress zone was a region of the stress-strain diagram in which gradual cavities were destroyed in a layer by layer manner. The size of this area depends on the percentage of porosity of the scaffold and the amount of its cavities. The slope of the curve in the first area, which was linear, showed the amount of the elastic coefficient.

As shown in Figure 5, the addition of 20% by weight of akermanite nanoparticles to the polylactic acid scaffold significantly increased the strength (the compressive strength of the

PLA scaffold was about 24.9 MPa); the compressive strength of the PLA-Ak scaffold was about 33.8 MPa. This increase was due to the strengthening effect of the akermanite particles. As can be seen from Figure 5, the addition of nanoparticles had a slight effect on the elastic coefficient of the scaffold. In general, the improvement in the mechanical properties of a composite depends on the physical properties of its filler, such as particle size, particle shape and dimensional ratio. Also, the distribution and dispersion of particles in the field and the interaction between the particles and the polymer could affect the final properties of the composite. Decreasing the particle size from micrometer to nanometer could have a significant effect on improving the properties of polymer-based composites [18].

3-5- Bioactivity test

Bioactivity of substances is usually done by immersing them in the simulated body fluid (SBF). Due to the immersion of the sample in the SBF, hydroxyapatite crystals are formed on the surface of the implant, indicating the bioactivity of its surface; it this causes the implant to connect with the living tissue [19]. In this experiment, the prepared scaffolds were immersed in the SBF solution for 4 weeks and bioactivity was examined by forming apatite on the surface of the scaffolds at the intervals of one week using the scanning electron microscopy.

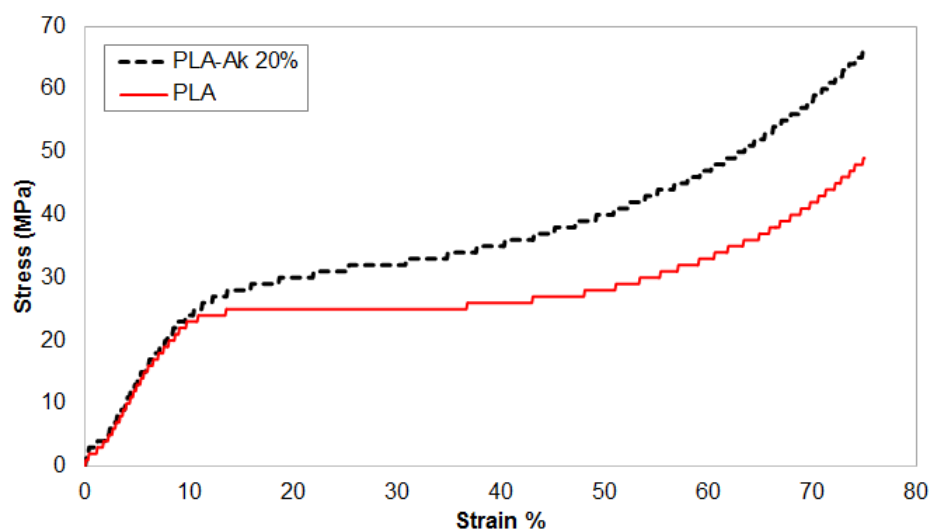


Fig. 5. Stress-strain curves of the PLA and PLA-Ak scaffolds compression test.

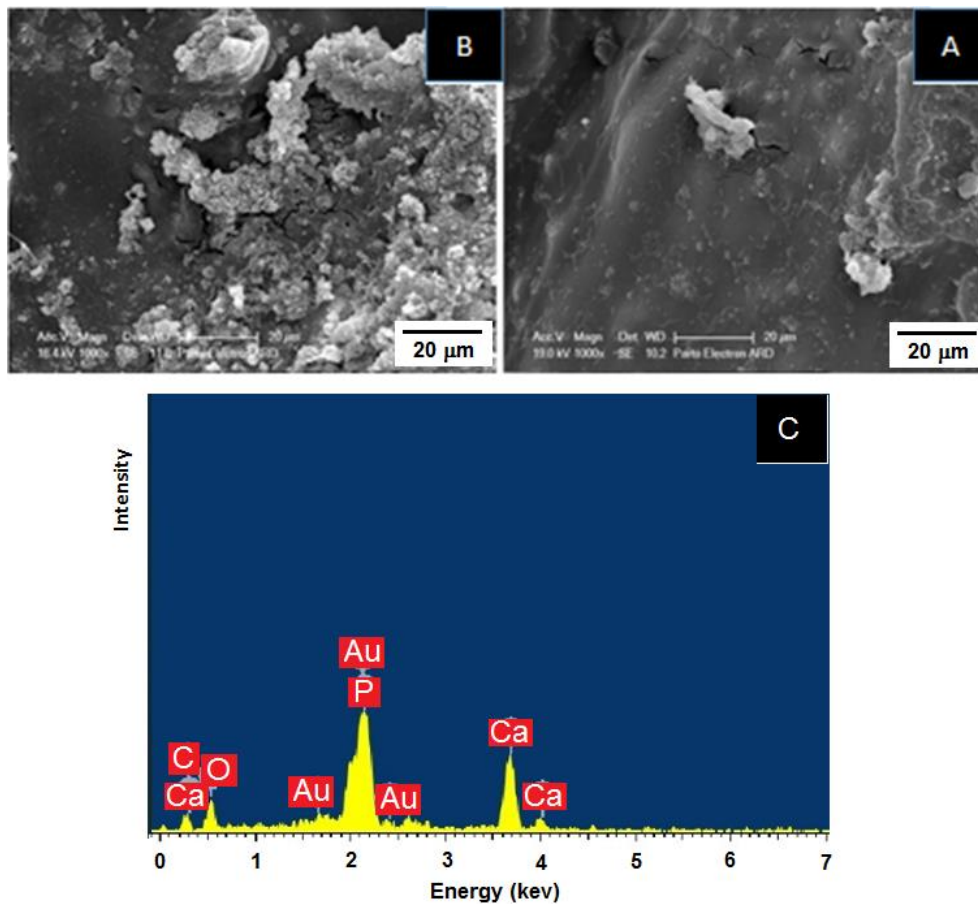


Fig. 6. Scanning electron microscopy (SEM) image of the surface of the nanocomposite scaffolds: A) PLA and B) PLA-Ak after four weeks of immersion in the SBF.

Figure 6 shows the images of the scanning electron microscopy of the scaffold surfaces. As can be seen, apatite crystals were formed on the surface of the scaffold containing akermanite nanoparticles; with increasing the immersion time in the SBF solution, the amount of the apatite crystals formed on the scaffold surface was increased. However, there was no apatite on the surface of the PLA scaffold. Deng et al. also showed that akermanite deposited apatite on the surface of the scaffold [6], which could be regarded as an important factor in the bone regeneration [6]. Akermanite has also been considered for its high capability of apatite deposition and its ability to induce the bone formation by the release of the soluble ions (Ca, Mg and Si) [13, 20, 21].

In addition to large apatite crystals, small particles of apatite were also seen in some places, indicating the germination of new mineral particles. Leonor et al. also showed that as the immersion time in the SBF solution was increased, the number and size of Ca-P nucleus on the biometric surface were raised as well; they became larger by sticking to each other.

The crack observed in the apatite layer was due to the shrinkage, which, in turn, could be attributed to the drying of the scaffold surface after leaving the SBF solution. These apatites are grown in specific places where the germination site is heterogeneous [20].

4-Conclusion

In this study, PLA nanocomposite scaffolds containing akermanite particles were prepared using the FDM technology. Akermanite particles were identified by electron microscopy (TEM) and X-ray diffraction (XRD); the results confirmed the formation of akermanite nanoparticles. Scanning electron microscopy (SEM) images showed the formation of the scaffold with interconnected pores, which would be suitable for the penetration of oxygen and nutrients and the disposal of waste from the tissue. The distribution of nanoparticles was investigated using electron microscopy with field emission (FESEM) and EDXA (map) of the silicon element, showing a uniform distribution of nanoparticles. The results of the compression test also revealed that adding 20%

by weight of the akermanite nanoparticles increased the strength of the polylactic acid polymer scaffold. Immersion of the scaffolds nanocomposite in the SBF solution after almost one month indicated the formation of hydroxyapatite crystals on the surface of the scaffolds.

4. References

1. R. Langer, Perspectives and challenges in tissue engineering and regenerative medicine, *Advanced Materials* 21(2009) 3235–3236.
2. E. Boccardi, I. V. Belova, G.E. Murch, A.R. Boccaccini, T. Fiedler, Oxygen diffusion in marine-derived tissue engineering scaffolds, *Journal of Materials Science: Materials in Medicine* 26 (2015) 1–9.
3. S. Yang, H. Yang, X. Chi, J.R.G. Evans, I. Thompson, R.J. Cook, P. Robinson, Rapid prototyping of ceramic lattices for hard tissue scaffolds, *Materials and Design* 29 (2008) 1802–1809.
4. C.C. Esposito, F. Gervaso, F. Scalera, F. Montagna, T. Maiullaro, A. Sannino, A. Maffezzoli, 3D printing of hydroxyapatite polymer-based composites for bone tissue engineering, *Journal of Polymer Engineering* 37 (2017) 741–746.
5. D.M. Correia, C. Ribeiro, V. Sencadas, L. Vikingsson, M.O. Gasch, J.L.G. Ribelles, G. Botelho, S. Lanceros-méndez, Strategies for the development of three dimensional scaffolds from piezoelectric poly (vinylidene fluoride), *Materials and Design* 92 (2016) 674–681.
6. Y. Deng, M. Zhang, X. Chen, X. Pu, X. Liao, Z. Huang and G. Yin, A novel akermanite/poly (lactic-co-glycolic acid) porous composite scaffold fabricated via a solvent casting-particulate leaching method improved by solvent self-proliferating process, *Regenerative Biomaterials*, (2017) 233–242.
7. S. Naghieh, M.R. Karamooz Ravari, M. Badrossamay, E. Foroozmehr, M. Kadkhodaei, Numerical investigation of the mechanical properties of the additive manufactured bone scaffolds fabricated by FDM: the effect of layer penetration and post-heating, *Journal of the Mechanical Behavior of Biomedical Materials* 59 (2016) 241 – 250.
8. S. Naghieh, A. Reihany, A. Haghghat, E. Foroozmehr, M. Badrossamay, F. Forooghi, Fused Deposition Modeling and Fabrication of a Three-dimensional Model in Maxillofacial Reconstruction, *Regeneration, Reconstruction & Restoration* 1 (2016) 139–144.
9. S. Naghieh, M. Badrossamay, E. Foroozmehr, M. Kharaziha, Combination of PLA Micro-fibers and PCL-Gelatin Nano-fibers for Development of Bone Tissue Engineering Scaffolds, *International Journal of Swarm Intelligence and Evolutionary Computation* 6 (2017) 1-4.
10. A. S. Zanetti, Characterization of Novel Akermanite: Poly-E-Caprolactone Scaffolds for Bone Tissue Engineering Applications Combined with Human Adipose-Derived Stem Cells, *LSU Doctoral Dissertations* (2011).
11. C. E. Corcione, F. Gervaso, F. Scalera, S. K. Padmanabhan, M. Madaghiele, F. Montagna & A. Maffezzoli, Highly loaded hydroxyapatite microsphere/PLA porous scaffolds obtained by fused deposition modelling. *Ceramics International* 45(2) (2019) 2803-2810.
12. E. Nejati, H. Mirzadeh, M. Zandi, Synthesis and characterization of nano-hydroxyapatite rods/poly(l-Lactide acid) composite scaffolds for bone tissue engineering , *Composites: Part A*, 39 (2008) 1589-1596.
13. C.Y. Tang, D.Z. Chen, T.M. Yue, K.C. Chan, C.P. Tsui, Peter H.F. Yu, Water absorption and solubility of PHBV/HA nanocomposites, *Composites Science and Technology* 68 (2008) 1927–1934.
14. S. J. Kalita, A. Bhardwaj & H. A. Bhatt, Nanocrystalline calcium phosphate ceramics in biomedical engineering. *Materials Science and Engineering: C*, 27(3) (2007) 441-449.
15. T. Kokubo, H. Takadama, How useful is SBF in predicting in vivo bone bioactivity?, *Biomaterials* 27 (2006) 2907–2915.
16. A. A. Najafinezhad, M. Abdollahi, H. Ghayour, A. Soheily, A. Chami , A. Khandan, A comparative study on the synthesis mechanism, bioactivity and mechanical properties of three silicate bioceramics, *Materials Science and Engineering C* 72 (2017) 259 –267.
17. Implants for surgery - In vitro evaluation for apatite-forming ability of implant Materials, *INTERNATIONAL STANDARD, ISO/FDIS 23317, 2007 (E)*.
18. U. Kneser, D.J. Schaefer, E. Polykandriotis et al. Tissue engineering of bone: the reconstructive surgeon's point of view. *Journal of Cellular and Molecular Medicine* 10 (2006) 7–19.
19. I. B., Leonor, A. Ito, K. Onuma, N. Kanzaki, and R. L. Reis In vitro bioactivity of starch thermoplastic/hydroxyapatite composite biomaterials: An in situ study using atomic

- force microscopy. *Biomaterials* 24 (2003) 579-585.
20. A Saadat, A.A. Behnamghader, S. Karbasi, D. Abedi, M. Soleimani, Comparison of acellular and cellular bioactivity of poly 3-hydroxybutyrate/hydroxyapatite nanocomposite and poly 3-hydroxybutyrate scaffolds, *Biotechnology and bioprocess engineering* 18 (3) 587-593.
21. N. Zhang, H.L. Nichols, S. Tylor, X. Wen, Fabrication of nanocrystalline hydroxyapatite doped degradable composite hollow fiber for guided and biomimetic bone tissue engineering, *Materials Science and Engineering C* 27 (2007) 599–606.